R2R-Based Continuous Production of Patterned and Multilayered Elastic Substrates with Liquid Metal Wiring for Stretchable Electronics

*Hiroki Kawakami, Kyohei Nagatake, Sijie Ni, Fumika Nakamura, Tamami Takano, Koki Murakami, Ibuki Ohara, Yuji Isano, Ryosuke Matsuda, Hideki Suwa, Ryunosuke Higashi, Moeka Kanto, Masato Saito, Hajime Fujita, Takuto Araki, Shingo Ozaki, Kazuhide Ueno, Tatsuhiro Horii, Toshinori Fujie, and Hiroki Ota**

The roll-to-roll (R2R) process for fabricating elastic substrates is essential for the social implementation of next-generation stretchable devices with soft interfaces. In recent years, there is a growing demand for soft heterostructures with multiple monolithically patterned organic materials. However, a continuous processing technique for substrates with heterostructures patterned using highly stretchable wiring has not yet been developed. Conventional manufacturing methods for stretchable electronics lack production capacity. This study introduces an R2R-based method for the continuous production of multilayered substrates composed of various elastic materials, integrated with liquid metal (LM) wiring, suitable for stretchable electronics. Continuous fabrication of polymer films is achieved with pattern areas as small as 0.78 mm^2, using three different polymers varying in hardness. The R2R coating process, paired with liquid metal wiring dispensing printing, allows for the creation of lines as fine as 140 microns. This process supports the batch production of 15 stretchable hybrid devices at a time and enables the creation of large-area devices up to 400 cm^2. The fabrication technique developed herein holds promise for the future manufacturing of not only stretchable electronics but also cutting-edge soft electronics like smart packaging. This is expected to be a factor leading to the commercialization of stretchable electronics.

1. Introduction

The roll-to-roll (R2R) process has been used in the manufacturing industry as a processing method, primarily for newspapers, photographs, and packaging materials.[1,2] With the development of additional functionalities, such as the conductivity and semiconductivity of organic and inorganic inks, the R2R method is now applied as a processing method for advanced electronic devices and elements.[3–7] Recently, electronic devices have become increasingly flexible, and manufacturing using printing technology is inexpensive and highly compatible with flexible materials.[8] Therefore, the fabrication technology for R2R processing is used for developing flexible electronic substrates, displays, organic solar cells, and biosensors.[9–13] In addition, elastic materials such as silicone,[14,15] hydrogels,[16] and natural rubber[17] are

H. Kawakami, K. Nagatake, S. Ni, F. Nakamura, T. Takano, K. Murakami, I. Ohara, Y. Isano, R. Matsuda, H. Suwa, R. Higashi, H. Ota
Department of Mechanical Engineering
Yokohama National University
79-5 Tokiwadai, Hodogaya-ku, Yokohama, Kanagawa 240-8501, Japan
E-mail: ota-hiroki-xm@ynu.ac.jp

The ORCID identification number(s) for the author(s) of this article can be found under https://doi.org/10.1002/admt.202400487

DOI: 10.1002/admt.202400487

M. Kanto, K. Ueno
Department of Chemistry and Life Science
Yokohama National University
79-5 Tokiwadai, Hodogaya-ku, Yokohama, Kanagawa 240-8501, Japan

M. Saito, H. Fujita, T. Horii, T. Fujie
Department of Life Science and Technology
Tokyo Institute of Technology
4259 Nagatsuta-cho, Midori-ku, Yokohama, Kanagawa 226-8501, Japan

T. Araki, K. Ueno
Institute of Advanced Science
Yokohama National University
79-5 Tokiwadai, Hodogaya-ku, Yokohama, Kanagawa 240-8501, Japan

T. Araki
Faculty of Engineering
Yokohama National University
79-5 Tokiwadai, Hodogaya-ku, Yokohama, Kanagawa 240-8501, Japan

used as stretchable substrates for fabricating next-generation electronic and stretchable devices that can reduce the load on biological tissues and improve followability. Processing these stretchable materials using the R2R process is an effective approach to enable the mass and large-area production of electronic devices for social implementation.

Coating technologies based on the R2R process, such as gravure coating[18] and blade coating,[19] have been used as continuous manufacturing methods for substrates comprising a single stretchable material. Furthermore, by combining the R2R process with printing technologies such as, rotary screen printing[20] and inkjet printing,[21] not only a continuous manufacturing method for stretchable substrates but also continuous manufacturing of wiring has been realized. Thus, the R2R process for stretchable materials has been developed to a technological level sufficient for manufacturing stretchable substrates and their circuits made of a single material. In recent years, the need for substrate materials with monolithic patterns and multilayered structures of multiple stretchable materials for stretchable devices has increased.

Although stretchable sensors and devices are currently being developed,[22–29] it is difficult to fabricate highly integrated electric circuits on stretchable substrates. Recently, stretchable hybrid devices have been developed to replace some functions of conventional solid-state electronic devices.[30] Because solid-state circuit elements are used, it is necessary to use a structure that suppresses tension on the elements. Substrates with a hard–soft structure with multiple layers of hard and soft organic materials in a pattern are used as stretchable substrates.[31] Patterned substrates and sheets with monolithic multilayers of organic materials can be considered not only for stretchable electronics but also for soft robots, smart packaging, and industrial processes.[32–35] However, the fabrication of stretchable substrates with hard and soft structures requires complicated processing methods, such as molding, photolithography, and annealing, owing to the need to prevent delamination between layers under tension by strengthening the adhesion between hard and soft layers.[36–39] Furthermore, the materials used for stretchable electrodes must have high elasticity because stress concentration occurs near the boundary between the soft and hard layers in these multilayered stretchable substrates. However, an R2R-based continuous fabrication process for multilayer patterned stretchable substrates that satisfy these wiring requirements has not yet been established.

Therefore, in this study, we proposed an R2R-based continuous production method for multilayered and patterned substrates made of stretchable organic materials with liquid metal (LM) wiring. Furthermore, as a proof-of-concept for processing stretchable hybrid devices, solid-state electronic devices were mounted on circuit boards fabricated using the proposed production method, resulting in the batch production of multiple and large stretchable hybrid devices. The R2R process for substrate fabrication includes a two-step R2R process with a gravure coater to create a release layer and a knife coater capable of corona pretreatment to improve the adhesion of the multilayer structure made of polymer materials. The intermediate- and hard-layer patterns on the soft layer were fabricated by attaching a mask and using a knife as a squeegee. Circuit patterns made of liquid metal which has significantly high stretchability were printed onto the fabricated substrates using a dispenser. This combination of printing technologies enables the continuous production of multilayers and patterned stretchable substrates with liquid metal wiring. Furthermore, by mounting solid electronic elements and packaging the elastic material with a spray coater, the printing process of stretchable hybrid devices for batch production and the fabrication of large devices was demonstrated. The production method was proposed as a fundamental technology for substrate and sheet fabrication in stretchable electronics, soft robotics, smart packaging, and industrial processes, and we believe that this technique will contribute to the progress of social implementation in these areas.

2. Result and Discussion

2.1. Stretchable Hybrid Devices Fabricated using the R2R Process

In this study, we developed a technique for the continuous fabrication of patterned multilayered and stretchable substrates using the R2R process. Furthermore, the batch production and scale-up of stretchable hybrid devices using this process were validated as a proof-of-concept. The proposed stretchable hybrid device consists of a soft layer substrate made of silicone elastomer (Eco-flex), a patterned intermediate layer made of polydimethylsiloxane (PDMS), a patterned hard layer made of epoxy, solid-state electronic components, liquid metal wiring, and packaging with Eco-flex (**Figure 1**a,b). As shown in Figure 1a, the solid-state electronic component was placed in the epoxy section to prevent stress loading on the device during large deformation. The remaining components of the device were composed of a large deformable silicone elastomer (Eco-flex) and a stretchable electrode (liquid metal; Galinstan) to keep the device stretchable. The fabricated stretchable hybrid device is shown in Figure 1bi, wherein the rigid solid-state electronic device is placed in the hard-layer portion and liquid metal wiring is connected to the components (Figure 1bii). 3D interconnections were fabricated by applying a stretchable insulator (silicone) to the liquid metal to prevent the liquid metal from electrical crossing (Figure 1biii). When more complex circuits are to be mounted, a flexible substrate on which electronic elements are mounted can be directly mounted onto a stretched substrate (Figure 1biv).

S. Ozaki
Division of System Research, Faculty of Engineering
Yokohama National University
79-5 Tokiwadai, Hodogaya-ku, Yokohama, Kanagawa 240-8501, Japan
T. Fujie
Research Center for Autonomous Systems Materialogy (ASMat)
Institute of Innovative Research
Tokyo Institute of Technology
R3-23, 4259 Nagatsuta-cho, Midori-ku, Yokohama, Kanagawa 226-8501, Japan
H. Ota
Graduate School of System Integration
Yokohama National University
79-5 Tokiwadai, Hodogaya-ku, Yokohama, Kanagawa 240-8501, Japan
H. Ota
Institute for Multidisciplinary Sciences
Yokohama National University
79-5 Tokiwadai, Hodogaya-ku, Yokohama, Kanagawa 240-8501, Japan

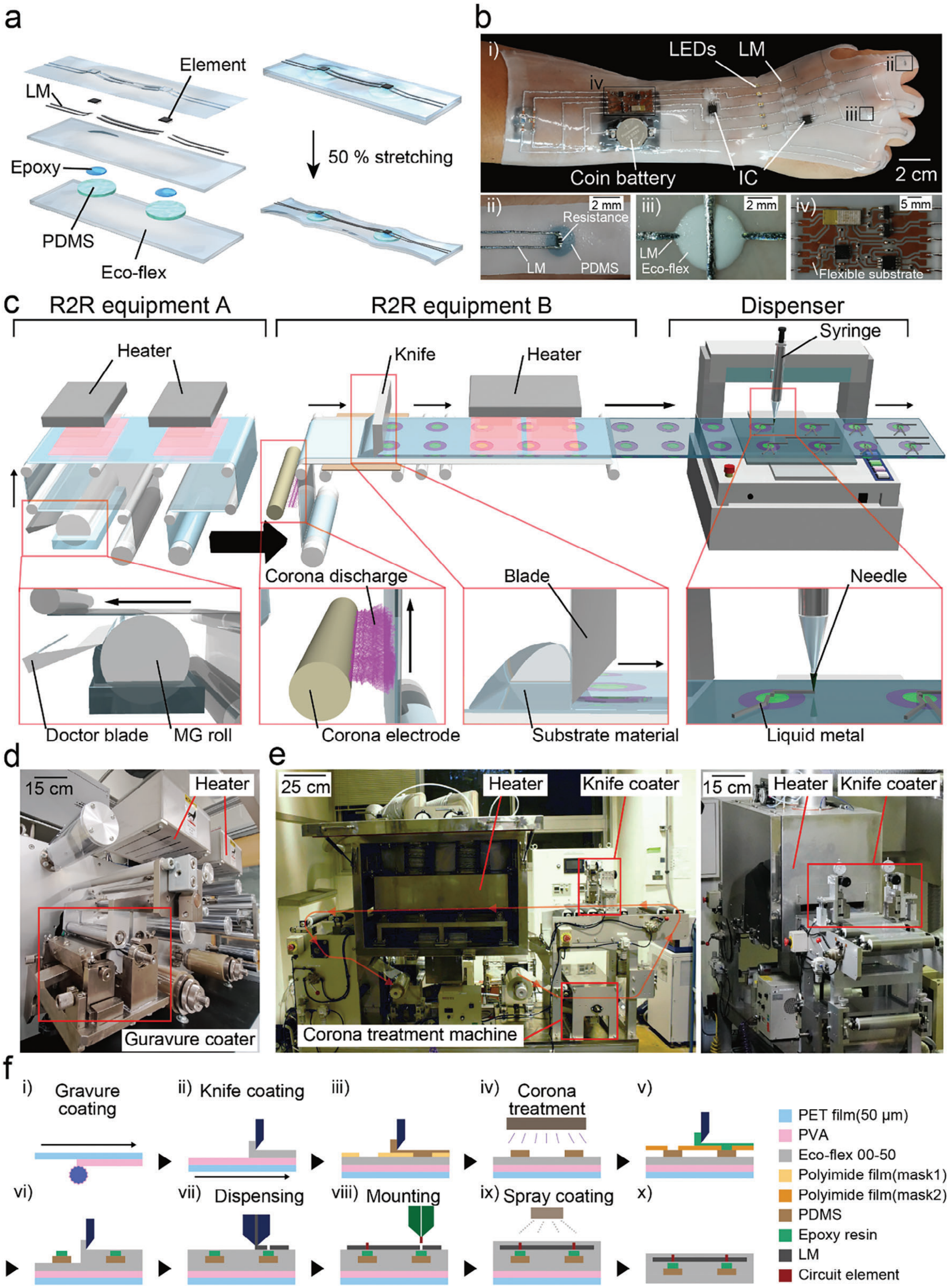

Figure 1. Stretchable hybrid devices fabricated using the R2R-based method. a) Internal structure of the stretchable hybrid device. The patterned PDMS and epoxy layers are fabricated inside Eco-flex packaging, which is capable of large deformation, to prevent the deformation of solid-state electronic elements while maintaining the stretchability of the device using liquid metal as wiring. b) Large-area wearable stretchable hybrid device. c) Concept of continuous production of patterned multilayer stretchable substrates using gravure and knife coaters based on the R2R process and dispensers. d) Rotogravure coater equipment based on the R2R process (R2R process equipment (A)). e) Knife coater equipment based on the R2R process with corona treatment machine (R2R process equipment (B)). f) Process for fabricating stretchable hybrid devices.

The continuous production of patterned multilayer stretchable substrates consists of three types of printing: a patterned multilayer stretchable substrate fabrication process using gravure coating for the ultrathin release layer of the multilayered substrate (R2R process equipment (A)), knife coating to fabricate the multilayered substrate in the R2R process (R2R process equipment (B)), and patterning of liquid metal wiring using a dispensing process (Figure 1c). Practically, the R2R and dispensing processes can be used for fabricating several components, ranging from the substrate to circuit wiring, through continuous production. Finally, to construct the device, the solid-state electrical components were mounted using a mounter, and the entire device was packaged with a spray coater.

The gravure and knife coaters used in this study are shown in Figure 1d,e, and Figure S1 (Supporting Information). The R2R process equipment (A) comprises a gravure coater and a heater. The gravure coater can produce thin films of 20 nm or more[40] using the micro gravure (MG) roll, as shown in Figure 1d and Figure S1a (Supporting Information). The pre-cured layer coated on the polyethylene terephthalate (PET) film was formed in a heater and collected on a rewinding roll. The R2R process equipment (B) (Figure 1e) comprises a corona treater, knife coater, and heater. It has a minimum and maximum coating speed of 0.1 and 1.0 m min^{-1}, respectively. Compared with the gravure coater, the knife coater can coat materials with a higher viscosity and adjust the film thickness.[9,40] In the R2R process, which is generally used to produce thin films by transfer,[41] it is challenging to achieve uniform patterning with the film thickness produced in this study. To achieve uniform patterning, knife coating, which was used in this study, and slot die coating, wherein the material is discharged from a blade, are suitable. The corona treater improved the wettability of polymer materials through surface activation via corona discharge (Figure S1b, Supporting Information).

The actual process of fabricating stretchable hybrid devices using this equipment is as follows: to facilitate the peeling of the fabricated patterned multilayer stretchable substrate, polyvinyl alcohol (PVA) was coated using the gravure coater of the R2R process equipment (A) (Figure 1fi). Eco-flex, a soft basal layer material of the patterned multilayer stretchable substrate, was prepared using the knife coater of the R2R process equipment (B) (Figure 1fii). To create the patterned PDMS interlayer, a polyimide (PI) mask was attached before coating, and the PDMS monomer was applied using the knife coater and polymerized using the heater (Figure 1fiii). The minimum gap between PDMS patterns and the reproducibility of the pattern diameter depended on the mask. After performing corona treatment to improve the wettability of the PDMS layer (Figure 1fiv), another PI mask was attached, and the epoxy resin, as the hard layer material, was coated using the knife coater in the same manner as that used for coating the intermediate PDMS layer and then cured (Figure 1fv). In this case, the patterning alignment was performed using alignment marks on the masks (Figure S2, Supporting Information). First, an L-shaped alignment mark was coated on the outside of the substrate area with PDMS, and then, the alignment mark on the masks for epoxy was applied to the mark on the Eco-Flex fabricated with PDMS to align the pattern. Because the surface of epoxy resin becomes spherical after curing, it is challenging to perform further patterning coatings on the epoxy resin surface. To ensure the flatness of the substrate, Eco-flex was coated after the coating of the three layers and polymerized (Figure 1fvi). After substrate fabrication, liquid metal wiring using a dispenser (Figure 1fvii), mounting circuit elements using a die bonder (Figure 1fviii), spray coating Eco-flex as packaging (Figure 1fix), and peeling the device from the PET substrate (Figure 1fx) were conducted in this order.

2.2. R2R Processing for Patterned Multilayer Stretchable Substrates

The processing characteristics of the PVA sacrificial layer coated by the gravure coater and the three-layer formation of Eco-flex (soft layer), PDMS (middle soft layer), and epoxy resin (hard layer) coated using the knife coater were investigated. A total of 4 patterned multilayer stretchable substrates consisting of three layers each of Eco-flex, PDMS, and epoxy are shown in **Figure 2a**. As shown in Figure 2a, a PDMS intermediate layer of 50.2 mm^2 and an epoxy layer of 12.6 mm^2 were formed on the Eco-flex substrate, which was laminated in a three-layer structure (Figure 2b).

In this study, an ultrathin PVA film was used as the sacrificial layer to detach the three-layer integrated structure of Eco-flex, PDMS, and epoxy from PET film. The thicknesses of the PVA films were determined based on the detachability of the three-layer product. Figure S3 (Supporting Information) shows the thickness of the PVA film fabricated using the gravure coater as well as the maximum peeling force of Eco-flex from a PET film at different PVA concentrations (5, 10, 15, and 20 wt%). As the PVA concentration increased, the PVA film thickness increased and the force required to peel Eco-flex decreased. The thicker the PVA layer, the more easily the Eco-flex substrate detaches from the PVA layer by absorbing more atmospheric moisture.[42,43] For the gravure-coated layers, there was a high correlation between the concentration and the film thickness;[44,45] therefore, the obtained film thickness data were reasonable. However, as shown in Figure S4 (Supporting Information), when the thick PVA layer significantly lowered the peeling force, the entire substrate was inadvertently removed along with the mask during the PDMS and epoxy patterning process. Based on the consideration of the peeling force, a PVA concentration of 10 wt.% was used to ensure stable peeling.

Figure S5 (Supporting Information) illustrates the relationship between the coating gap and film thickness for stretchable substrate materials such as Eco-flex, PDMS, and epoxy resin, over a gap range of 200–1400 µm using a knife coater. The coating film thickness was determined by the coating gap of the knife coater, coating speed, material viscosity, and surface tension between the material and substrate. The film thickness of Eco-flex and PDMS demonstrated high correlation with the coating gap, with coefficients of 0.991 and 0.992, respectively. For epoxy resin, however, film thickness was specifically measured at the pattern's center, revealing a trend where the pattern diameter expanded with increasing coating gaps. This led to a deviation from the linear thickness increase, likely due to the epoxy spreading under its own weight at wider gaps, which resulted in an unexpectedly thinner central film. Under the conditions of this study, a coating gap of approximately 100 µm was determined as the

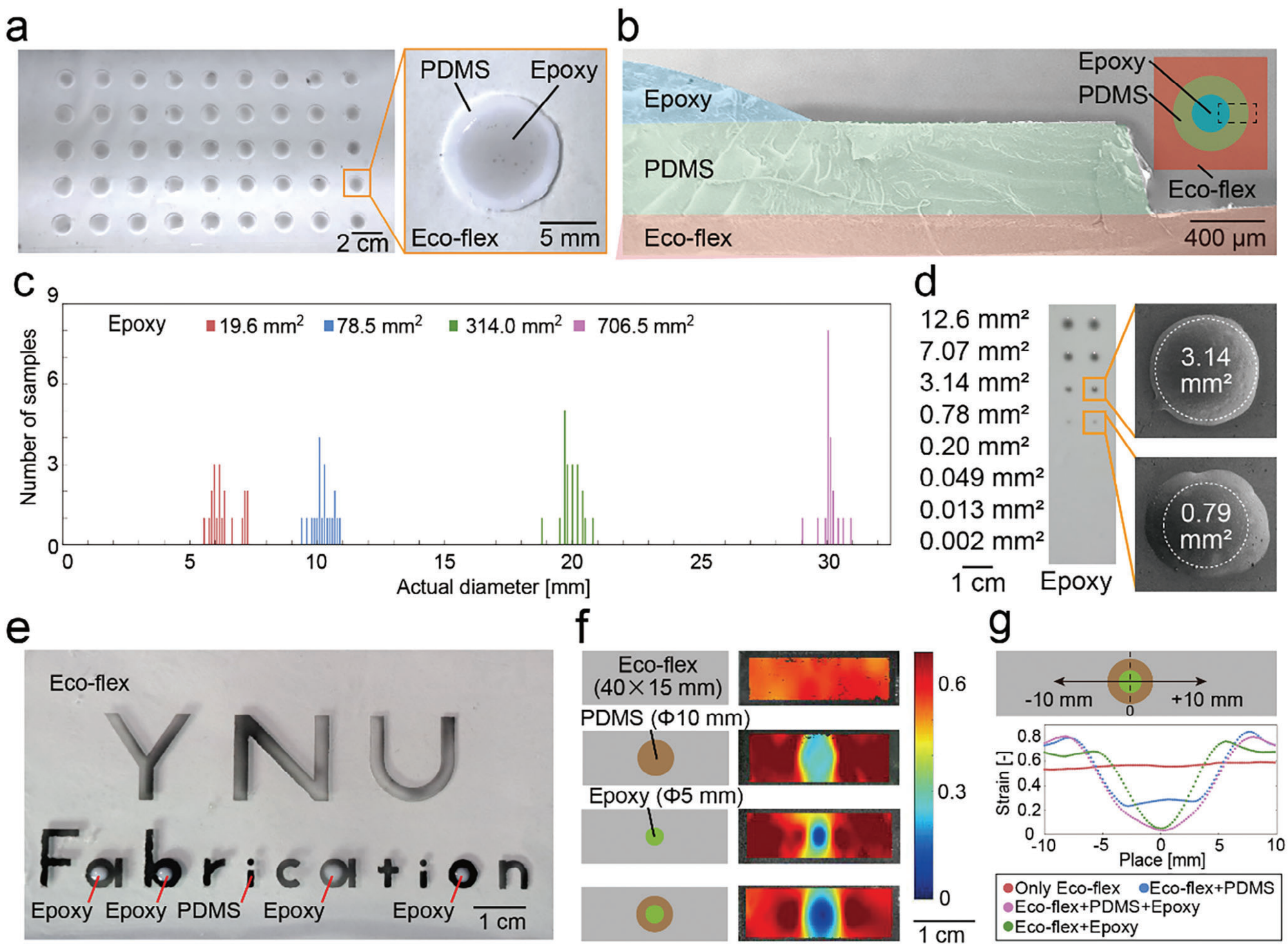

Figure 2. a) Large-area substrate with 45-segment hard and soft patterns. b) Cross section of hard and soft patterns captured using the scanning electron microscope. The bottom layer is Eco-flex (a soft elastomer), the middle layer is PDMS, and the top layer is epoxy resin. c) Production variation of circular epoxy patterns of 19.6, 78.5, 314.0, and 706.5 mm^2. d) Photographs of circular epoxy patterns of 12.6–0.002 mm^2 and their enlarged images. e) Demonstration of multilayered patterns of Eco-flex, PDMS, and epoxy resin. The pattern indicates a YNU pattern. f) Digital image correlation of three different substrates elongated with Eco-flex only, Eco-flex and PDMS, epoxy resin and Eco-flex, and Eco-flex, PDMS, and epoxy resin. g) Strain in the tensile direction ±10 mm from the center of the pattern.

coating limit. This is related to the surface tension of the material, and the coating limit can be adjusted by changing the material.

Next, we investigated substrate surface conditions that are crucial for fabricating epoxy resin and PDMS patterns. High adhesion between the silicone PDMS and phenolic epoxy layers was vital for continuous production, which we achieved by integrating a corona discharge mechanism into the roll-to-roll (R2R) system for sustained substrate surface activation. This improved the adhesion by increasing the PDMS surface energy and decreasing its contact angle with epoxy, as evidenced by Figure S6 (Supporting Information). Consequently, stable fabrication of large patterns, up to 201 mm^2, was demonstrated in Figure S7 (Supporting Information), despite the challenges posed by thermal shrinkage of epoxy and related stress.

The pattern diameter distributions of the circular patterns of 19.6, 78.5, 314.0, and 706.5 mm^2 of the epoxy resin and PDMS are shown in Figure 2c and Figure S6 (Supporting Information). The error of the 5-mm diameter epoxy resin pattern was ±0.7 mm, which was caused by diffusion owing to the weight of the thick film relative to the pattern diameter (Figure 2c). By contrast, the PDMS pattern error was ±0.023 mm (Figure S8, Supporting Information). The results of examining the minimum pattern sizes of the epoxy resin and PDMS are shown in Figure 2d and Figure S9 (Supporting Information), respectively. Figure S10 (Supporting Information) shows a high-magnification view of the patterns of epoxy resin and PDMS. From these results, patterns with minimum sizes up to 3.14 mm^2 for epoxy resin and 0.78 mm^2 for PDMS could be fabricated.

Using these techniques, arbitrary patterns were fabricated, as shown in Figure 2e. The substrate used was Eco-flex, the letters were made of colored PDMS, and epoxy was circularly patterned at the centers of a, b, and o. This ensured a high degree of freedom of pattern design.

Figure 2f illustrates the strain distribution under 50% tensile stress across different structures: Eco-flex alone, a two-layer combination of Eco-flex and PDMS, a similar two-layer combination of Eco-flex and epoxy, and a three-layer structure incorporating

Eco-flex, PDMS, and epoxy. The Eco-flex-only and Eco-flex-PDMS structures exhibited uniform extension, including at the center. In contrast, the Eco-flex-epoxy and the three-layer structures showed non-uniform stretching, with the epoxy layer remaining unstretched. Significantly, the inclusion of a PDMS intermediate layer moderated the tensile strain, preventing localized high stress, as further detailed in Figure 2g.

As the amount of heat generated by devices increases with the sophistication of stretchable electronics, thermal problems are expected to arise owing to the low thermal conductivity of stretchable substrates. The silicone material used as a substrate has low thermal conductivity, leading to such thermal problems because the generated heat cannot be dissipated and is stored. This study did not examine thermal problems because the temperatures were not sufficiently high to affect device functionality; however, in the field of stretchable electronics, it is necessary to develop appropriate heat dissipation technology to deal with such problems in the future.

Table S1 (Supporting Information) presents a summary of the features of stretchable devices employing rigid-soft structures, which are categorized into three types: 1) combinations of two soft elastomers bonded by high-affinity resins, such as Eco-flex with PDMS; 2) a pairing of a soft elastomer like Eco-flex with hard resins, including SU-8 and PLA;[46–49] and 3) a novel three-layer structure introduced in this study, consisting of a soft elastomer base, an intermediate layer, and a rigid top layer.

The first type of a rigid-soft structure, consisting of two soft elastomers, allows the device to maintain a high elongation of more than 100%. However, the hard elastomeric part of the substrate is elongated by approximately 7% of the total device elongation.[50] Therefore, it is difficult to directly mount electrical components made of thin metal films, such as thin-film transistors, onto a substrate.

In the second type, a substrate made of a soft elastomer and a hard resin, deformation of the hard resin portion can be suppressed to almost 0%. By contrast, the low adhesion between the hard resin and the elastomer and the high local stress at the boundary suppress the maximum elongation rate of the entire device and make the boundary area easy to break.

For these reasons, in the substrate consisting of three layers, the soft elastomer and intermediate layer can be used to maintain the maximum elongation rate of the entire device while suppressing breakage in elongation by placing the intermediate layer. Recently, a three-layer structure of Eco-flex-PDMS-PES (Polyethersulfone) and PDMS-PMMA (Polymethylmethacrylate)-Ni/PDMS/Si resin (OE6630) was reported.[39,51] With this structure, the deformation of the hard-layer portion can be suppressed to approximately 0% while maintaining approximately 100% expansion of the entire device. The structure fabricated in this study also achieved a maximum elongation rate of 265%, and an examination using the digital image correlation (DIC) confirmed that deformation in the higher layers could be suppressed to less than 4%, which is equivalent to the performance of the devices fabricating using manual substrate processing. The ability to both maintain the maximum elongation rate and form a deformation region close to 0% is considered to be a significant advantage when considering future high-performance thin-film electronic devices to be mounted directly on substrates.

By using the R2R process proposed in this study, it was possible to fabricate several patterns within a few steps. However, the minimum pattern area was 0.78 mm^2, which is less than the minimum size achieved through the existing manual substrate fabrication methods (Table S1, Supporting Information).[46,48] This issue should be addressed in future studies.

Regarding the manufacturing variation, the average errors of the 19.6-mm^2 epoxy resin and PDMS patterns were 7.6% and 1%, respectively. This accuracy may be sufficient for fabricating the substrate. Furthermore, it has been reported that, the larger the scale of production, the smaller the manufacturing pattern error.[52] Therefore, the patterning method proposed in this study may have had a smaller error owing to further large-scale production.

2.3. 2D/3D Liquid Metal Wiring by the Dispensing Process

The liquid metal wiring patterns used in this study were fabricated on Eco-flex using the liquid metal Galinstan with a dispenser. The dispensing area was 30 × 30 cm^2, but when combined with the processing area of the R2R process, the wiring area in this study was 12 × 30 cm^2. Changes in the resistance of liquid metal wiring and a stretchable electrode made of a mixture of Ag flakes and styrene butadiene styrene (SBS; polystyrene-block-polybutadiene-block-polystyrene) when a maximum of 50% tensile force was applied are shown in **Figure 3a**. In the elastic wiring using liquid metal, the change in resistance was 0.08 Ω at the first 50% pull, and the conductivity was maintained even after stretching 100 times of 50% stretching, whereas the resistance of the silver paste increased by 463 MΩ at approximately 10% of the tensile force. Because the surface tension of the liquid metal is related to the adhesive strength with the substrate, the peel strength between the wiring and substrate was not examined.

In this study, liquid metal was used as the conductive material for stretchable electrodes. The conductive material used for stretchable electrodes in other studies is a silver paste, which is a mixture of silver flakes, silver particles,[53] and silver nanowires[54] in a stretchable polymer and liquid metal.[55] Galinstan, a type of liquid metal, is a gallium-based material with an electrical conductivity of 3.1 × 10^6 S m^{-1} and a melting point of −19 °C.[56] At the current values used in general wearable devices, such as those studied herein, the liquid metal wiring is stable and unaffected. Although gallium is a rare metal and inexpensive, the resistance of liquid metal wiring can be suppressed to a change of approximately 0.967% per 1% strain, and electrodes with sufficient conductivity have been reported, even when strains of approximately 200% are applied.[57] However, it has been reported that silver paste, which utilizes the percolation phenomenon, exhibits a resistance change of approximately 2.5% per 1% strain.[58] Liquid metal can adapt to physical shape changes caused by mechanical deformation and has self-healing capability;[59] therefore, it retains conductivity even when repeatedly stretched. The resistance of the silver paste in the static state changes owing to the cycles of expansion and contraction caused by the plastic deformation of the silver paste substrate. However, the resistance of liquid metal in the static state does not change unless the substrate on which

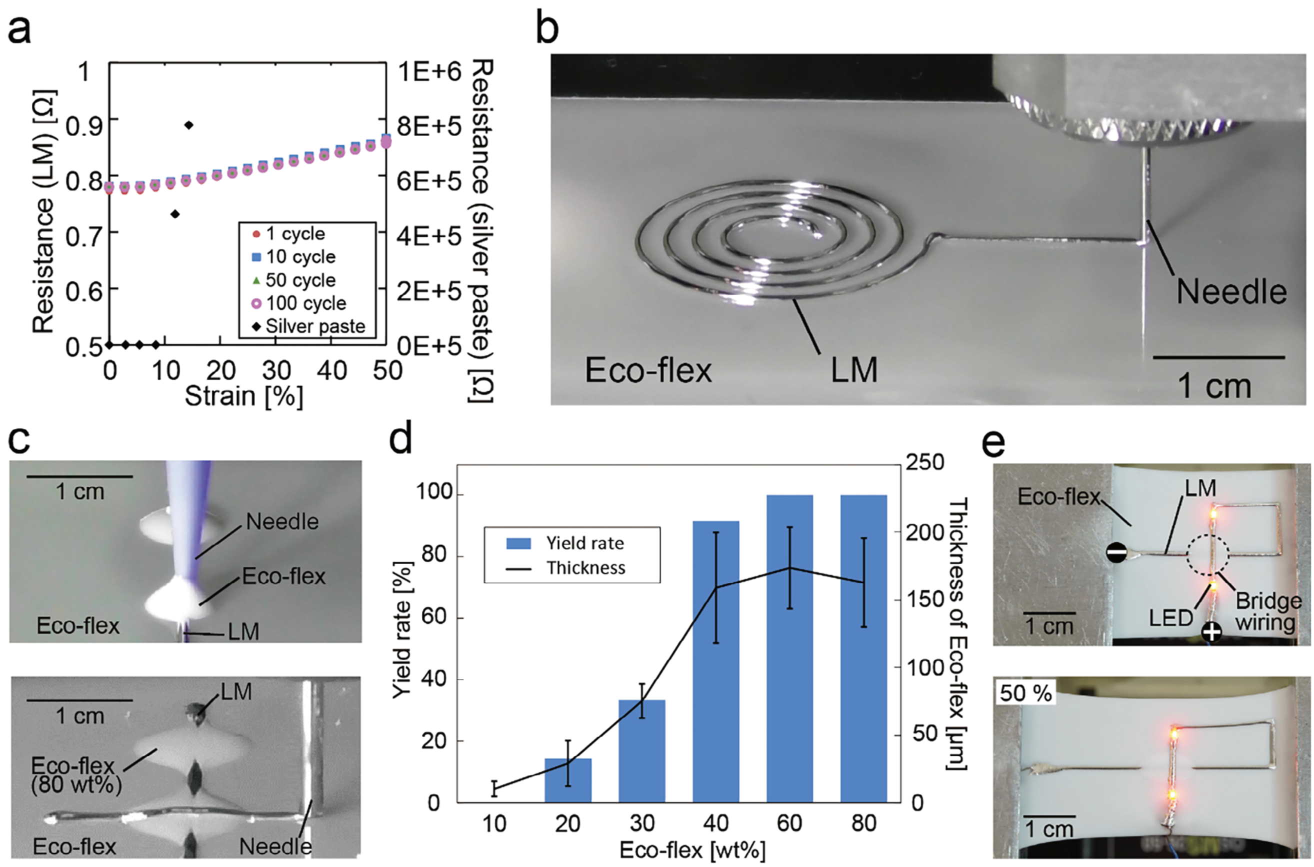

Figure 3. Characterization of 2D/3D liquid metal wiring fabricated using the dispensing process. a) Changes in resistance when 100 cycles of 50% stretching are applied to the liquid metal wiring and the changes in silver paste wiring when pulled until it is broken. b) Image of spiral-shaped wiring. c) Image of the fabrication process of 3D liquid metal wiring. d) Relationship between the concentration of Eco-flex used for the encapsulation of liquid metal wiring and the film thickness of the encapsulation layer and the yield rate of insulation for the two intersecting wires at each concentration. e) Image showing insulation properties under stretching.

the liquid metal is applied is plastically deformed. Therefore, liquid metals have very high electrical stability against large deformations.

The controllability of the wiring width and 3D images according to the needle diameter are shown in Figures S12–S14 (Supporting Information). The 3D shape of the liquid metal was not completely semicircular or arch-shaped but flattened at the top because the liquid metal was applied using a dispenser. The top surface of the liquid metal wiring has a wall-like edge arising from the excess liquid metal discharged during wiring. However, this did not affect the conductive function. These liquid metal interconnections were not encapsulated. As shown in Figure S14 (Supporting Information), the linewidth of liquid metal wiring was controlled by the nozzle diameter. The minimum line width was 140 µm with a 180-µm needle tip in this experimental setup (Figures S12 and S15, Supporting Information). Increasing the diameter of the liquid metal wiring is facile. However, wires with larger diameters are more easily affected by the fluidity of the liquid metal; therefore, it may be appropriate to use a liquid metal paste composed of oxidized Ga or In, Ni powder, Cu powder, and SiO_2 powder to suppress fluidity. As shown in Figure 3b, a liquid metal can be depicted with a high degree of freedom in a 2D depiction.

Screen printing,[60] lift-off, lithography,[61] and dispensing[62] methods are available as wiring methods for liquid metals. Screen printing methods are simple, but their accuracy is limited to approximately 30 µm.[60] Combined lift-off and lithography method can depict patterns of 0.180 µm, but is not suitable for continuous production.[61] The dispensing method allows a direct depiction of the designed pattern without masks or molds. It has been reported that wiring with a minimum line width of 1.9 µm can be fabricated.[62] These dispenser-based methods are promising for achieving both ultrafine lines and continuous production, although they have some limitations such as the inner diameter of the nozzle, nozzle-to-substrate distance, and printing speed.[62]

The 3D wiring is indispensable for circuit fabrication, and 3D wiring using a liquid metal was performed in this study. After the liquid metal wiring was created, a polymerized encapsulation layer was created by adding Eco-flex using a dispenser, and the liquid metal wiring was further depicted on the encapsulation layer (Figure 3c). The viscosity of Eco-flex was lowered using hexane to ensure stable dispensing using the dispenser used in this study. Figure 3d shows the film thickness of each Eco-flex-encapsulated layer and the yield rate (n = 12) of the 3D liquid metal wiring when using each Eco-flex-encapsulated layer. In particular, when the Eco-flex concentration exceeds 60%, 3D wiring can be fabricated with a yield rate of 100%. We fabricated a circuit that emitted light from two light-emitting diodes (LEDs) using 3D wiring (Figure 3e; Figures S16 and S17, Supporting Information). In a circuit such as that shown in Figure S16 (Supporting Information), when the 3D wiring fails (Figure S17, Supporting Information), the two electrodes are shorted, and the LED does not emit light. As shown in Figure 3e, the circuit was successfully fabricated, and the two LEDs emitted light.

In this study, 3D wiring using liquid metal can be broadly classified into two types: 3D wiring without a supporting material and 3D wiring with a supporting material such as an insulator or Eco-flex. Fabrication of wiring without an insulator has been reported to utilize the shape retention property of the liquid owing to the oxide film of the liquid metal,[62,63] and has the advantage of simplifying the fabrication process. The developed method involves installing an insulator, that is, Eco-flex, between the electrodes, as used in conventional solid-state electronic devices. Although more processes are required, 3D wiring with an insulator was used in this study, considering the stability of the device, Eco-flex,[64] PDMS,[64] poly(styrene-ethylene/butylene-styrene) (SEBS),[65] and Perfluoropolyether (PFPE-) diols[66] are commonly used as stretchable insulators for the 3D interconnections. Among these, Eco-flex was used to achieve the adhesion and stretchability of the substrate in this study. However, it is generally difficult to form ultrathin submicron films with good insulation properties owing to the film formation method and wettability of rubber materials. Therefore, achieving stretchable ultrathin films with insulating properties must be studied in future research. In addition, the dispensing system is a point manufacturing method, making it an even more efficient continuous manufacturing process. Therefore, the potential of this R2R process to be used for the liquid metal interconnection process should be considered as a future study. For this purpose, the application of the printing technique for conductive materials[20,67–71] to R2R is expected to develop into a continuous fabrication technology for liquid metal interconnections.

The R2R process and dispensing process shown in Figures 2 and 3, respectively, will enable the continuous fabrication of stretchable devices that have thus far been fabricated manually. Therefore, our manufacturing process is different from previously developed manufacturing processes, and is expected to be a factor leading to the commercialization of stretchable electronics.

2.4. Batch Production of Stretchable Hybrid Devices

To demonstrate the R2R manufacturing and dispensing processes, multiple stretchable devices were produced in batches. **Figure 4a** shows the production of 15 stretchable hybrid devices in one batch, including the system and sensors. Conventional manufacturing processes for stretchable devices, such as spin-coating, screen-printing, bar-coating, and photolithography,[72] are not continuous processes; only one to several devices can be fabricated in a single process. In comparison, our R2R process provides an advantage in terms of mass production. The number of devices produced in a single process can be varied depending on the size of the device. Figure S18 (Supporting Information) shows the circuit diagram of the manufactured devices. The illuminance of the LEDs on the device changed to red, green, or blue, depending on the illuminance measured by the photodetector on the circuit. The LEDs turned red when the illuminance was 2059–3219 lx, green when the illuminance was 1205–2059 lx, and blue when the illuminance was 45–1205 lx. To achieve a standalone operation, a flexible battery was installed behind the flexible board. Fifteen devices were manufactured in a single production run.

Figure 4b shows the results of pulling the device under 2400 lx illumination with an LED on the device lit red. Figure 4c shows the results when the devices were exposed to light at 2400 lx, 1490 lx, and 430 lx with 70% stretching (Figure 4b; Video S1, Supporting Information). As shown in Figure 4c and Video S2 (Supporting Information), the color of the LED changed according to the illuminance.

When the entire device was elongated by 70%, the strain was approximately 200% in the Eco-flex part and 0% in the flexible substrate part (Figure 4d). This result indicates that the displacement in the flexible substrate portion is suppressed, and that the entire device is stretched when elongation occurs in the liquid metal wiring and Eco-flex portions. The change in the voltage applied to the phototransistor when the displacement was applied was measured (Figure 4e). Because the rate of change of the voltage value was at most 1%, we confirmed that there was no effect of the change on the resistance of the wiring owing to tension and that the measurement performance of the phototransistor was not affected.

Furthermore, the change in the wiring width under tension in the area of liquid metal wiring was connected to a flexible substrate using two types of substrates: a hard and soft pattern substrate composed of Eco-flex and PDMS and an Eco-flex substrate only (Figure 4f). In the case of the hard and soft pattern substrate, the wiring width in the connection area remained within the range of 99–102% compared with the original state, even when tension was applied, therefore, the wiring width was stable (Figure S19a,b, Supporting Information). However, in the device with the flexible substrate directly placed on the Eco-flex substrate, the wiring width decreased linearly after the displacement started, and the wiring was disconnected when the stress was more than 50% (Figure S19c, Supporting Information). The standard deviation of the voltage value calculated from the irradiance was approximately 9% (Figure 4g). Finally, the fabricated device was attached to the human elbow, which has the largest skin expansion and contraction in the human body. The device functioned stably without damage when the elbow was bent and stretched under conditions in which each LED was lit (Figure 4h; Video S3, Supporting Information). These considerations enable the continuous manufacture of stretchable devices, facilitating the commercialization of the field of stretchable electronics, which is the emphasis of this study. A process to manufacture a large number of small devices based on large-area fabrication is important for the widespread adoption of the field of stretchable electronics.

In stretchable hybrid devices with flexible substrates placed on patterned multilayer stretchable substrates, as performed in this study, the maximum tensile strain of the entire device ranges from 30 to 60%,[30,73–75] and the local strain is approximately 40%.[75] In this study, we achieved a gloss elongation rate of more than 70%. The difference in the elongation rates was determined

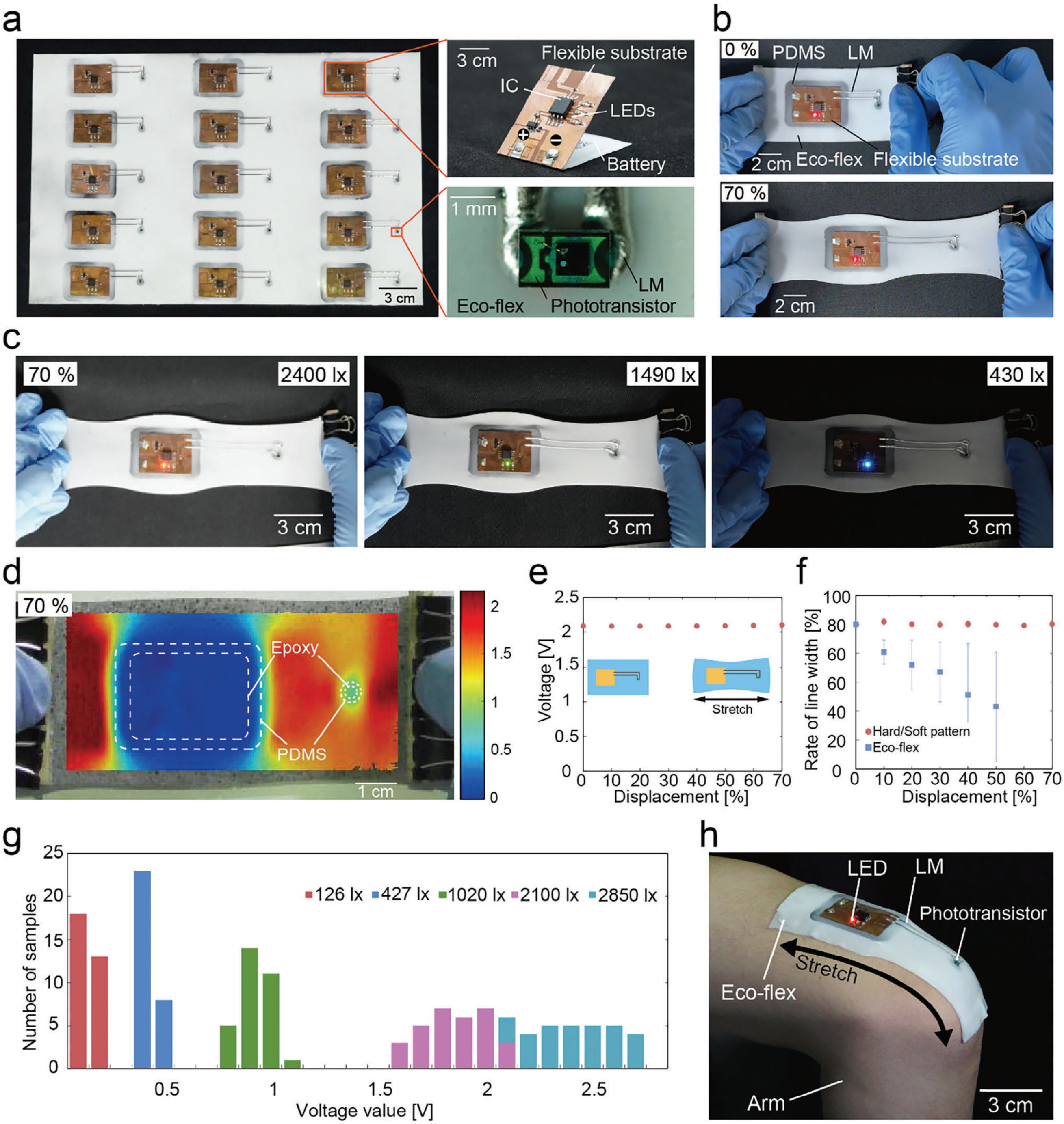

Figure 4. Batch production of multiple stretchable hybrid devices and the evaluation of fabricated devices. a) Batch production of 15 devices. A phototransistor is connected to the liquid metal on a rigid-soft-structured substrate; LEDs light up according to the amount of light received by the phototransistor. To enable a standalone operation, a flexible battery is mounted on the back of the flexible substrate. b) The device at 0% and 70% extension; emission of LEDs is stable at 70% extension and the device is still under function. c) The device at 70% extension with varying LED luminous intensities of 2400 lx, 1490 lx, and 430 lx; LEDs emit red, green, and blue lights at luminous intensities of 2059–3219 lx, 1205–2059 lx, and 45–1205 lx, respectively. d) Strain distribution when the device is elongated by 70%, with 200% elongation in the Eco-flex part and no deformation in the flexible substrate and sensor part. e) The voltage at the phototransistor part when the device is elongated by 0–70%, showing that the voltage is stable at 70% elongation. f) Line width variation in the connection part between the flexible substrate and the liquid metal wiring when the device is elongated by 0–70% using two types of substrates: rigid-soft pattern substrate and Eco-flex substrate. The use of a rigid-soft pattern effectively suppresses the shrinkage of the liquid metal wiring width at the flexible board connection. g) Voltage values at the phototransistor part when the device is exposed to light at five different illuminance levels (126, 427, 1020, 2100, and 2850 lx). h) The device when worn at the elbow.

by the area ratio of the flexible substrate to the stretched substrate. Therefore, depending on the application, the design must be optimized to determine the proportion of flexible substrates to be used for the entire area.

Solid-metal stretchable wiring with geometric patterns, such as meander structure wiring, has often been used as wiring in stretchable hybrid devices.[30,76,77] A few studies reported that these solid metal-based stretchable wirings tend to show large fluctuations in resistance and break at 60% tensile strain,[78,79] whereas, other studies reported that the liquid metal achieves more than 200% extension.[80] However, in the present study, the liquid metal was in a highly fluid liquid state, and the wiring broke by 50% tension when a direct flexible substrate was mounted on the stretched substrate. To prevent this rupture, a rigid-soft substrate comprising three layers was used in this study. Because this phenomenon can be mitigated using a liquid metal paste made by mixing Ni particles with liquid metal in the wiring,[81] stretchable hybrid devices that are more stable against expansion and contraction may be realized in the future using this liquid metal paste. The liquid metal paste may be used to realize stretchable hybrid devices that are more stable against expansion and contraction.

2.5. Demonstration of the Large-Area Stretchable Hybrid Device

A large-area stretchable device was fabricated, which was a stretchable temperature measurement device with a length of 30 cm and a width of 12 cm (**Figure 5**a). This manufacturing area indicates that a larger area can be produced than that with conventional manufacturing processes for stretchable devices. The device was divided into 18 segments, each of which consisted of a thermistor, fixed resistor, and transistor connected by a liquid metal. An image and a circuit diagram of a single segment are shown in Figure 5b. The device was composed of an 18-segment active matrix with transistors to detect the divided voltage values of the thermistors in each segment. The temperature was calculated for each segment based on the divided voltage values of the thermistors of the six pixels in a row on which the gate of the MOSFET-N was turned on. The thermistors and transistors mounted on the epoxy resin maintained stable contact with the liquid metal wiring even at 50% stretching because the hard layer of epoxy resin had a significantly higher Young's modulus than those of Eco-flex and PDMS. The average values of the measured temperatures in the thermostatic chamber set at 20–55 °C are shown in Figure 5c,d. Figure 5c shows the temperature measured by thermocouples in the thermostatic chamber and the correlation coefficient between the measured temperature of the device and the temperature inside the thermostatic chamber was 0.999, which was significantly high and shows excellent tracking performance. As shown in Figure 5d, the absolute average error of the measured temperature was 0.08 °C when the temperature inside the thermostatic chamber was 20.0 °C. The variation in the measured temperature from one pixel to another was sufficiently small.

The temperature distributions of the device on the two hot plates are shown in Figure 5e. The temperature of each area on the plates was measured using thermocouples and compared with the temperatures measured using the developed device. By comparing the average values of the temperatures measured by the device and thermocouples, an error of 0.45 °C in the absolute value was found in the set temperature of the hot plate.

The temperature distributions of the device on the two hot plates are shown in Figure 5e. The temperature of each area on the plates was measured using thermocouples and compared with the temperatures measured using the developed device. By comparing the average values of the temperatures measured by the device and thermocouples, an error of 0.45 °C in the absolute value was found in the set temperature of the hot plate.

Figure 5f shows the temperature distribution in each segment of the device when hot air was applied to the devices with tensile strengths of 0% and 50% using a dryer. The device responded instantaneously to the application of hot air from the dryer, showing the diffusion of heat from areas where heat was concentrated (Video S4, Supporting Information). Furthermore, the device behaved in the same manner under 50% device tension compared with that when no tension was applied, confirming that the device functioned with and without tension.

In this study, an absolute average error of 0.45 °C was observed between the device and hot plate temperature settings. This error may be because of the presence of errors in the resistance values of individual thermistors. The thermistor used in this device has a ±5% error in resistance at 25 °C, which causes an error of approximately 1 °C in the measured temperature; therefore, the error in the measured temperature is within the error range of the thermistor resistance. In addition, in the already reported temperatures of the stretchable hybrid device, the measurement temperature accuracy was less than 1% error in resistance at 20 °C, and the correlation coefficient in the resistance change between the ambient temperature and the device was 0.998.[82] The accuracy of the proposed device is comparable to that of the aforementioned devices, and the proposed device is considered to have sufficient device functionality.

To confirm the stability of the wiring, a simple 2×2 active matrix circuit similar to the temperature measurement device was fabricated and subjected to repeated tensile tests. A thermistor was substituted with a fixed resistor to eliminate temperature variations, and the change in resistance at both ends was measured. Repeated tensile tests were conducted for 100 cycles at 50% tension. As shown in Figure S20 (Supporting Information), most of the errors for all four px were stable at approximately 1%, and tension did not affect the active matrix circuit. The liquid metal wiring connected to the device was also protected by a hard layer, and no tensile effects were observed.

As shown in Table S1 (Supporting Information), the maximum area of the stretchable hybrid devices fabricated using the conventional molding and spin-coating methods shown in Table S1 (Supporting Information) is approximately 100 cm^2. Inkjet printing is a system similar to a dispensing system and can mold larger ranges than this, but substrate fabrication methods have not kept pace with size requirements. The R2R process enables the same stretchable substrate fabrication techniques as those listed in Table S1 (Supporting Information) while achieving batch/large-area fabrication, and this is not possible with the other techniques. With the R2R process used in this study, it is theoretically possible to fabricate large-area stretchable hybrid devices with sizes exceeding 400 cm^2; however, at this stage, the

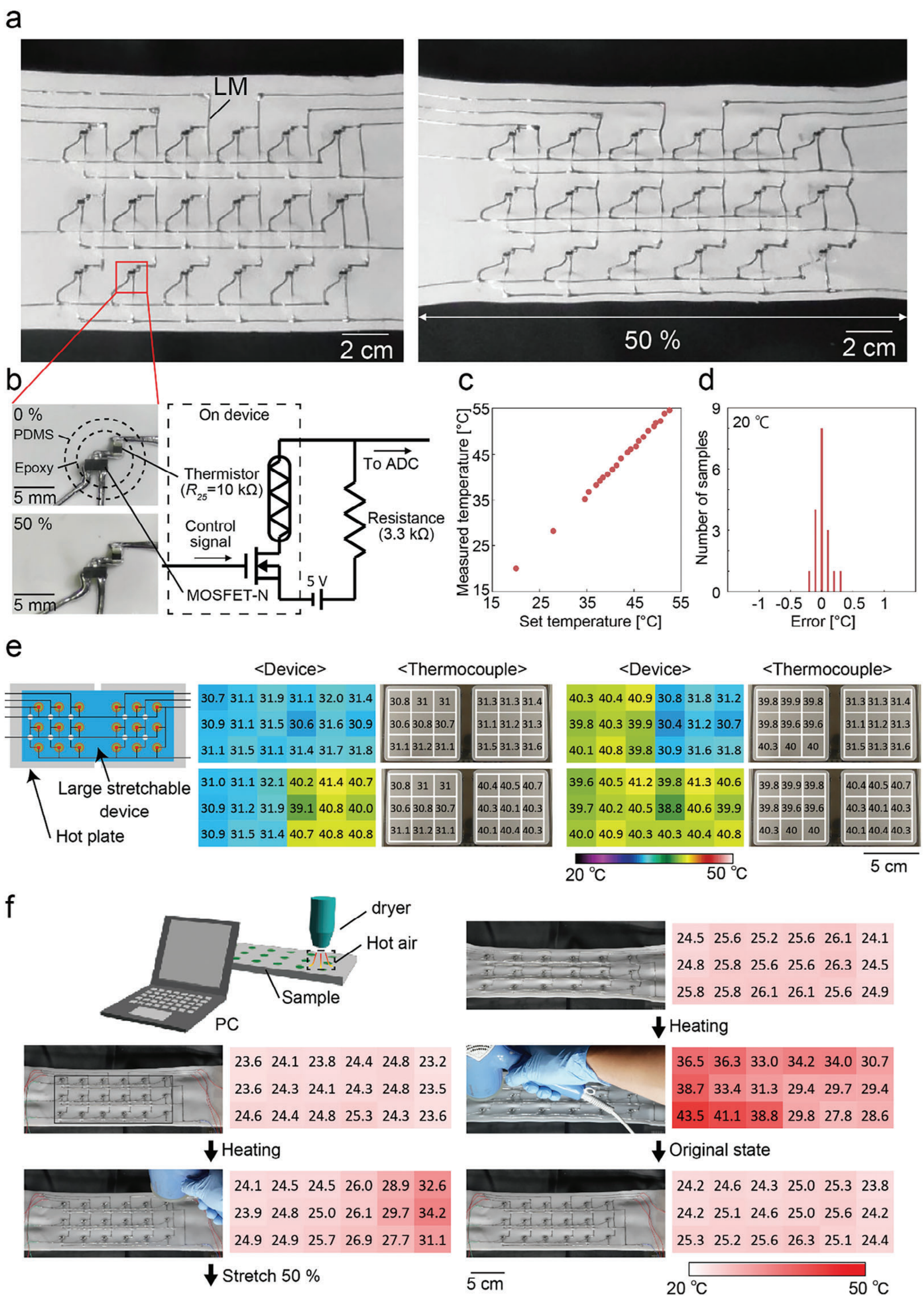

Figure 5. Large-area stretchable hybrid device capable of measuring temperature distributions and the evaluation of its function. a) Photograph of the large-area device in its original state and at 50% stretch. b) Magnified image of the hard and soft pattern areas in one segment and its circuit diagram. Displacement is not observed in the electric components of segment 1 when the device is expanded and contracted by 50% from the original state. However, the entire segment 1 is deformed by the deformation of the stretchable electrode. c) Relationship between the set environment temperature and the measured temperature for each segment. Segment 1 displays the temperature corresponding to the ambient temperature when the ambient temperature is set between 20 and 55 °C ($R^2 = 0.999$). d) Distribution of the measured temperature when the ambient temperature is 20.0 °C. The absolute mean error of the measured temperature is 0.08 °C. e) Temperature measurement evaluation of a large device in a static state. The temperature distribution is measured when the large device is placed on a hot plate and the temperature on the hot plate is changed to 30 °C and 40 °C. The temperatures are displayed in correspondence with the hot plate temperature. f) Real-time temperature display of each segment of the large device. It is demonstrated that the temperature can be measured in real time under conditions where the device is partially heated.

width is limited to 120 mm. The tensile limits listed in Table S1 (Supporting Information) were determined by the pattern width, pattern shape, and material properties of the hard-layer portion. In particular, the bond strength between the soft and hard layer portions is important to maximize material properties.

A method that can theoretically achieve a larger area has also been proposed by fabricating a rigid substrate containing solid elements and a substrate on which only the elastic wiring is mounted separately and connected together in arbitrary combinations similar to a puzzle.[83] This method can be used to fabricate large stretchable hybrid devices with high-definition patterns. By contrast, in this study, we fabricated devices with a size of 400 cm^2 using the R2R process. Using this method, it is possible to fabricate large stretchable hybrid devices with arbitrary hard and soft patterns in arbitrary locations and a high degree of freedom in the placement of solid-state electronic elements and stretchable wiring.

In the case of high-density integration of such multi-pixel devices, the current geometry is not suitable in terms of flexibility. However, the presence of a hard layer is necessary to realize a stable connection with the liquid metal wiring using hard circuit elements on a stretched substrate. In the future, it is necessary to fabricate devices with high integration by devising the shape of the hard layer and liquid metal interconnections. Stretchable circuit elements are necessary to achieve both integration and device stability. However, it is difficult to fabricate highly functional stretchable electronics because they tend to have inferior functionality compared with that of hard circuit elements.

3. Conclusion

In this study, a continuous processing method was developed to fabricate stretchable substrates of monolithic multilayered and patterned multiple organic materials with liquid metal wiring using a fabrication system combined with a printing process. In addition, batch production of stretchable hybrid devices and fabrication of large-area devices were performed using solid-state electrical component mounting and packaging. In the substrates, patterns of epoxy resin and PDMS were formed in multiple layers with a minimum area of 0.78 mm^2, and a continuous heteroelastic substrate that was stretchable throughout the device but not at the desired locations on the substrate was fabricated. Fifteen stretchable hybrid devices capable of light detection were produced in batch production. A light-detecting device that could emit red, green, and blue LED lights in response to light levels was fabricated, showing a sensitivity equivalent to that of the solid-state device. This functionality was maintained even when the device was further stretched by 70%. A stretchable hybrid device with an area of 400 cm^2 was fabricated. The transistor and thermistor were connected by liquid metal in one compartment, and 18 compartments were used to realize a device that could detect the temperature at each location on the device. The temperature of each compartment was displayed, and the temperature mapping on the device was confirmed. The accuracy of the device was also confirmed to be as sensitive as a solid-state thermistor. The above results demonstrate the superiority of the method reported in this study for the production of stretchable devices.

A method for fabricating patterned multilayer stretchable substrates with liquid metal wiring using an R2R-based process was developed, and batch production and large-area production of stretchable hybrid devices were conducted in this study. The minimum size of the pattern was 0.78 mm^2, and the challenge was to increase its resolution. To further refine the minimum 0.78-mm^2 pattern produced in this study, it is important to use methods such as gravure printing, inkjet printing, and flexographic printing, which are suitable for micropattern fabrication. Similarly, for liquid metal wiring, the current dispenser has a maximum fine line width of 140 μm, and further optimization of dispensing and R2R printing[73] will achieve continuous and highly fine liquid metal wiring. Currently, devices with limited functionality can be realized owing to their resolution; however, the technologies for a higher definition described above will contribute to the realization of high-performance stretchable hybrid devices, such as stretchable displays and smart packaging.

Supporting Information

Supporting Information is available from the Wiley Online Library or from the author.

Acknowledgements

H.K. and K.N. contributed equally to this work. This study was financially supported by the Japanese Science and Technology Agency (JST) Precursory Research for Embryonic Science and Technology (JPMJPR18J2), JST CREST (JP19209665), JST FOREST (JPMJFR203Q), and Grant-in-Aid for Scientific Research A (20H00213), and Scientific Research B (21H03815).

Conflict of Interest

The authors declare no conflict of interest.

Data Availability Statement

The data that support the findings of this study are available in the supplementary material of this article.

Keywords

elastic substrate, liquid metal, printing fabrication, roll-to-roll, stretchable electronics

Received: March 31, 2024
Revised: May 15, 2024
Published online:

[1] T. Mäkelä, T. Haatainen, P. Majander, J. Ahopelto, *Microelectron. Eng.* **2007**, *84*, 877.
[2] K. Maize, Y. Mi, M. Cakmak, A. Shakouri, *Adv. Mater. Technol.* **2023**, *8*, 2200173.
[3] C. Liedert, L. Rannaste, A. Kokkonen, O. H. Huttunen, R. Liedert, J. Hiltunen, L. Hakalahti, *ACS Sens.* **2020**, *5*, 2010.
[4] R. Abbel, Y. Galagan, P. Groen, *Adv. Eng. Mater.* **2018**, *20*, 1701190.
[5] H. Xin, W. Li, *Appl. Phys. Rev.* **2018**, *5*, 031105.
[6] S. Khan, S. Ali, A. Bermak, *Sensors* **2019**, *19*, 1230.

[7] A. C. O'Connor, T. J. Beaulieu, G. D. Rothrock, *NIST.GCR* **2016**, *16*, 008.
[8] A. M. Tiara, H. Moon, G. Cho, J. Lee, *Jpn. J. Appl. Phys.* **2022**, *61*, SE0802.
[9] R. R. Søndergaard, M. Hösel, F. C. Krebs, *J. Polym. Sci. B Polym. Phys.* **2013**, *51*, 16.
[10] H. Li, C. Zuo, A. D. Scully, D. Angmo, J. Yang, M. Gao, *Flex. Print. Electron.* **2020**, *5*, 014006.
[11] D. Wang, J. Hauptmann, C. May, Y. J. Hofstetter, Y. Vaynzof, T. Müller, *Flex. Print. Electron.* **2021**, *6*, 035001.
[12] M. Bariya, Z. Shahpar, H. Park, J. Sun, Y. Jung, W. Gao, H. Y. Y. Nyein, T. S. Liaw, L. C. Tai, Q. P. Ngo, M. Chao, Y. Zhao, M. Hettick, G. Cho, A. Javey, *ACS Nano* **2018**, *12*, 6978.
[13] J. Sun, A. Sapkota, H. Park, P. Wesley, Y. Jung, B. B. Maskey, Y. Kim, Y. Majima, J. Ding, J. Ouyang, C. Guo, J. Lefebvre, Z. Li, P. R. L. Malenfant, A. Javey, G. Cho, *Adv. Electron. Mater.* **2020**, *6*, 1901431.
[14] D. Qi, K. Zhang, G. Tian, B. Jiang, Y. Huang, *Adv. Mater.* **2021**, *33*, 2003155.
[15] N. Naserifar, P. R. LeDuc, G. K. Fedder, *Adv. Mater.* **2016**, *28*, 3584.
[16] S. Ding, Z. Jiang, F. Chen, L. Fu, Y. Lv, Y. Qian, S. Zhao, *ACS Appl. Mater. Interfaces* **2020**, *12*, 27572.
[17] M. Fan, L. Wu, Y. Hu, M. Qu, S. Yang, P. Tang, L. Pan, H. Wang, Y. Bin, *Adv. Compos. Mater.* **2021**, *4*, 1039.
[18] H. Kumagai, T. Fujie, K. Sawada, K. Takahashi, *Adv. Opt. Mater.* **2020**, *8*, 1902074.
[19] Y. Chen, Y. Guo, S. Batra, E. Unsal, E. Wang, Y. Wang, X. Liu, Y. Wang, M. Cakmak, *RSC Adv.* **2015**, *5*, 92071.
[20] O. H. Huttunen, T. Happonen, J. Hiitola-Keinänen, P. Korhonen, J. Ollila, J. Hiltunen, *Ind. Eng. Chem. Res.* **2019**, *58*, 19909.
[21] H. Ervasti, T. Järvinen, O. Pitkänen, É. Bozó, J. Hiitola-Keinänen, O. H. Huttunen, J. Hiltunen, K. Kordas, *ACS Appl. Mater. Interfaces* **2021**, *13*, 27284.
[22] S. Zeng, J. Zhang, G. Zu, J. Huang, *Carbohydr. Polym.* **2021**, *267*, 118198.
[23] S. M. Kim, H. J. Kim, H. J. Jung, J. Y. Park, T. J. Seok, Y. H. Choa, T. J. Park, S. W. Lee, *Adv. Funct. Mater.* **2019**, *29*, 1807760.
[24] J. Yan, Y. Xia, J. Lai, C. Zhao, D. Xiang, H. Li, Y. Wu, Z. Li, H. Zhou, *Macromol. Mater. Eng.* **2022**, *307*, 2100765.
[25] S. Guo, H. Xu, Y. Zheng, L. Li, Z. Li, L. Zhang, H. Zhang, X. Wang, J. Li, L. Wang, L. Liu, Z. Lou, *Nano Energy* **2023**, *110*, 108361.
[26] M. Hyouk Kim, M. Woo Jeong, J. Su Kim, T. Uk Nam, N. Thanh Phuong Vo, L. Jin, T. Il Lee, J. Young Oh, *Sci. Adv.* **2022**, *8*, eade2988.
[27] K. Sim, Z. Rao, H.-J. Kim, A. Thukral, H. Shim, C. Yu, *Sci. Adv.* **2019**, *5*, eaav5749.
[28] M. D. Dickey, *Adv. Mater.* **2017**, *29*, 1606425.
[29] C. Majidi, *Adv. Mater. Technol.* **2019**, *4*, 1800477.
[30] Y. S. Kim, M. Mahmood, Y. Lee, N. K. Kim, S. Kwon, R. Herbert, D. Kim, H. C. Cho, W. H. Yeo, *Adv. Sci.* **2019**, *6*, 1900939.
[31] B. Lee, H. Cho, S. Jeong, J. Yoon, D. Jang, D. K. Lee, D. Kim, S. Chung, Y. Hong, *J. Inf. Disp.* **2022**, *23*, 163.
[32] R. Lin, Y. Li, X. Mao, W. Zhou, R. Liu, *Adv. Mater. Technol.* **2019**, *4*, 1900614.
[33] H. Yu, Y. Lian, T. Sun, X. Yang, Y. Wang, G. Xie, X. Du, J. Gou, W. Li, H. Tai, *ACS Appl. Mater. Interfaces* **2019**, *11*, 43543.
[34] J. Kwon, Y. Takeda, R. Shiwaku, S. Tokito, K. Cho, S. Jung, *Nat. Commun.* **2019**, *10*, 54.
[35] Q. Chen, Z. Pei, Y. Xu, Z. Li, Y. Yang, Y. Wei, Y. Ji, *Chem. Sci.* **2018**, *9*, 623.
[36] S. Gandla, H. Gupta, A. R. Pininti, A. Tewari, D. Gupta, *RSC Adv.* **2016**, *6*, 107793.
[37] M. Zhu, Z. Sun, Z. Zhang, Q. Shi, T. He, H. Liu, T. Chen, C. Lee, *Sci. Adv.* **2020**, *6*, eaaz8693.
[38] X. Yu, X. Gong, C. Podder, B. Ludwig, I. M. Chen, W. Shou, A. Alvidrez, G. Chen, X. Huang, H. Pan, *Adv. Eng. Mater.* **2021**, *23*, 2100286.
[39] H. Park, K. Cho, H. Oh, S. Kim, *Superlattices Microstruct.* **2018**, *117*, 169.
[40] Y. Fu, E. G. Dudley, *Compr. Rev. Food Sci. Food Saf.* **2021**, *20*, 3404.
[41] R. Sondergaard, M. Hosel, D. Angmo, T. T. Larsen-Olsen, F. C. Krebs, *Mater. Today* **2012**, *15*, 1.
[42] H. Abral, A. Atmajaya, M. Mahardika, F. Hafizulhaq, Kadriadi, D. H., S. M. Sapuan, R. A. Ilyas, *J. Mater. Res. Technol.* **2020**, *9*, 2477.
[43] M. S. Peresin, Y. Habibi, A. H. Vesterinen, O. J. Rojas, J. J. Pawlak, J. V. Seppälä, *Biomacromolecules* **2010**, *11*, 2471.
[44] S. Schiessl, E. Kucukpinar, N. Rivollier, H.-C. Langowski, P. Eisner, *Polymers* **2023**, *15*, 2761.
[45] N. Sato, A. Murata, T. Fujie, S. Takeoka, *Soft Matter* **2016**, *12*, 9202.
[46] M. S. Lim, M. Nam, S. Choi, Y. Jeon, Y. H. Son, S. M. Lee, K. C. Choi, *Nano Lett.* **2020**, *20*, 1526.
[47] A. Romeo, Q. Liu, Z. Suo, S. P. Lacour, *Appl. Phys. Lett.* **2013**, *102*,131904.
[48] Y. Liu, Z. Liu, B. Zhu, J. Yu, K. He, W. R. Leow, M. Wang, B. K. Chandran, D. Qi, H. Wang, G. Chen, C. Xu, X. Chen, *Adv. Mater.* **2017**, *29*, 1701780.
[49] J. C. Yang, S. Lee, B. S. Ma, J. Kim, M. Song, S. Y. Kim, D. W. Kim, T.-S. Kim, S. Park, *Sci. Adv.* **2022**, *8*, 3863.
[50] W. Wang, S. Wang, R. Rastak, Y. Ochiai, S. Niu, Y. Jiang, P. K. Arunachala, Y. Zheng, J. Xu, N. Matsuhisa, X. Yan, S. K. Kwon, M. Miyakawa, Z. Zhang, R. Ning, A. M. Foudeh, Y. Yun, C. Linder, J. B. H. Tok, Z. Bao, *Nat. Electron.* **2021**, *4*, 143.
[51] J. Byun, E. Oh, B. Lee, S. Kim, S. Lee, Y. Hong, *Adv. Funct. Mater.* **2017**, *27*, 1701912.
[52] T. Happonen, T. Kokko, E. Juntunen, K. Rönk, *Flex. Print. Electron.* **2019**, *4*, 025002.
[53] H. J. Nam, Y. H. Hwangbo, S. Y. Nam, H. M. Nam, *Coatings* **2023**, *13*, 1499.
[54] R. Kawabata, T. Araki, M. Akiyama, T. Uemura, T. Wu, H. Koga, Y. Okabe, Y. Noda, S. Tsuruta, S. Izumi, M. Nogi, K. Suganuma, T. Sekitani, *Flex. Print. Electron.* **2022**, *7*, 044002.
[55] Y. Lee, D. S. Kim, S. W. Jin, H. Lee, Y. R. Jeong, I. You, G. Zi, J. S. Ha, *Chem. Eng. J.* **2021**, *427*, 130858.
[56] X. Wang, R. Guo, J. Liu, *Adv. Mater. Technol.* **2019**, *4*, 1800549.
[57] J. B. Chossat, Y. L. Park, R. J. Wood, V. Duchaine, *IEEE Sens. J.* **2013**, *13*, 3405.
[58] X. Li, X. Li, M. Wang, R. Zheng, Y. Jin, Z. Gu, *Chem. Eng. J.* **2023**, *471*, 144843.
[59] H. Wang, S. Chen, X. Zhu, B. Yuan, X. Sun, J. Zhang, X. Yang, Y. Wei, J. Liu, *Matter* **2022**, *5*, 2054.
[60] S. P. Sreenilayam, I. U. Ahad, V. Nicolosi, V. Acinas Garzon, D. Brabazon, *Mater. Today* **2020**, *32*, 147.
[61] M. gu Kim, D. K. Brown, O. Brand, *Nat. Commun.* **2020**, *11*, 1002.
[62] Y.-G. Park, H. S. An, J.-Y. Kim, J.-U. Park, *Sci. Adv.* **2019**, *5*, eaaw2844.
[63] C. Ladd, J. H. So, J. Muth, M. D. Dickey, *Adv. Mater.* **2013**, *25*, 5081.
[64] J. Yoon, S. Y. Hong, Y. Lim, S.-J. Lee, G. Zi, J. S. Ha, *Adv. Mater.* **2014**, *26*, 6580.
[65] Y. Li, N. Li, W. Liu, A. Prominski, S. Kang, Y. Dai, Y. Liu, H. Hu, S. Wai, S. Dai, Z. Cheng, Q. Su, P. Cheng, C. Wei, L. Jin, J. A. Hubbell, B. Tian, S. Wang, *Nat. Commun.* **2023**, *14*, 4488.
[66] J. Liu, J. Wang, Z. Zhang, F. Molina-Lopez, G. J. N. Wang, B. C. Schroeder, X. Yan, Y. Zeng, O. Zhao, H. Tran, T. Lei, Y. Lu, Y. X. Wang, J. B. H. Tok, R. Dauskardt, J. W. Chung, Y. Yun, Z. Bao, *Nat. Commun.* **2020**, *11*, 3362.
[67] T. Kaneko, Y. F. Wang, M. Hori, T. Sekine, A. Yoshida, Y. Takeda, D. Kumaki, S. Tokito, *Adv. Mater. Technol.* **2023**, *8*, 2300436.
[68] S. H. Jeong, A. Hagman, K. Hjort, M. Jobs, J. Sundqvist, Z. Wu, *Lab Chip* **2012**, *12*, 4657.

[69] S. H. Jeong, K. Hjort, Z. Wu, *Sci. Rep.* **2015**, *5*, 8419.
[70] B. Wang, W. Xin, K. Hjort, C. Guo, Z. Wu, A. C. S. Appl, *Polym. Mater.* **2019**, *1*, 145.
[71] S. Zhang, B. Wang, J. Jiang, K. Wu, C. F. Guo, Z. Wu, *ACS Appl. Mater. Interfaces* **2019**, *11*, 7148.
[72] D. C. Kim, H. J. Shim, W. Lee, J. H. Koo, D.-H. Kim, *Adv. Mater.* **2020**, *32*, 15.
[73] M. Miyakawa, H. Tsuji, M. Nakata, *J. Soc. Inf. Disp.* **2022**, *30*, 699.
[74] H. Li, Y. Xu, X. Li, Y. Chen, Y. Jiang, C. Zhang, B. Lu, J. Wang, Y. Ma, Y. Chen, Y. Huang, M. Ding, H. Su, G. Song, Y. Luo, X. Feng, *Adv. Healthcare Mater.* **2017**, *6*, 1601013.
[75] X. Li, M. M. Hasan, H. M. Kim, J. Jang, *IEEE Trans. Electron Devices* **2019**, *66*, 2971.
[76] J. Van Den Brand, M. De Kok, M. Koetse, M. Cauwe, R. Verplancke, F. Bossuyt, M. Jablonski, J. Vanfleteren, *Solid State Electron* **2015**, *113*, 116.
[77] J. A. Rogers, T. Someya, Y. Huang, *Stem Cells Int.* **2010**, *327*, 1603.
[78] C. F. Li, W. Li, H. Zhang, J. Jiu, Y. Yang, L. Li, Y. Gao, Z. Q. Liu, K. Suganuma, *ACS Appl. Mater. Interfaces* **2019**, *11*, 3231.
[79] A. M. Yunos, G. Omar, H. A. Hamid, M. A. Salim, N. A. Masripan, *J. Phys. Sci.* **2020**, *31*, 75.
[80] C. Votzke, U. Daalkhaijav, Y. Git Mengüç, M. L. Johnston, *IEEE Sens. J.* **2019**, *19*, 3832.
[81] M. S. Kim, S. Kim, J. Choi, S. Kim, C. Han, Y. Lee, Y. Jung, J. Park, S. Oh, B. S. Bae, H. Lim, I. Park, *ACS Appl. Mater. Interfaces* **2022**, *14*, 1826.
[82] S. Y. Hong, Y. H. Lee, H. Park, S. W. Jin, Y. R. Jeong, J. Yun, I. You, G. Zi, J. S. Ha, *Adv. Mater.* **2016**, *28*, 930.
[83] J. Kang, D. Son, O. Vardoulis, J. Mun, N. Matsuhisa, Y. Kim, J. Kim, J. B. H. Tok, Z. Bao, *Adv. Mater. Technol.* **2019**, *4*, 1800417.

